



# Coexistence of superconductivity and ferromagnetism in $\text{La}_{1.85}\text{Sr}_{0.15}\text{CuO}_4\text{--La}_{2/3}\text{Sr}_{1/3}\text{MnO}_3$ matrix composites

Xuecan Yao, Yuan Jin, Mingtao Li, Zhe Li, Guixin Cao, Shixun Cao, Jincang Zhang\*

Department of Physics, Shanghai University, Shanghai 200444, China

## ARTICLE INFO

### Article history:

Received 6 November 2010

Received in revised form 22 February 2011

Accepted 22 February 2011

Available online 1 March 2011

### PACS:

74.72.Dn

74.62.Dh

74.25.Fy

75.47.Lx

### Keywords:

Cuprate superconductor

Ferromagnetic manganites

Matrix composites

Coexistence of ferromagnetism and superconductivity

## ABSTRACT

In order to clarify the interaction between superconductivity and magnetism, a series of  $(\text{La}_{1.85}\text{Sr}_{0.15}\text{CuO}_4)_{1-x}(\text{La}_{2/3}\text{Sr}_{1/3}\text{MnO}_3)_x$  matrix composites ( $x = 0\text{--}0.2$ , mole fraction) was successfully prepared by solid-state reaction method. Based on the electrical transport measurements, it is found that the superconductivity is gradually suppressed as increasing the content of  $\text{La}_{2/3}\text{Sr}_{1/3}\text{MnO}_3$  (LSMO) manganites and that the superconductivity still exists in the composites even though plenty of LSMO is introduced into  $\text{La}_{1.85}\text{Sr}_{0.15}\text{CuO}_4$  (LSCO) superconducting cuprate. At the same time, the results of the magnetic measurements also demonstrate the coexistence between superconductivity and ferromagnetism when the  $\text{CuO}_2$  planes are intact as follows from the results of X-ray diffraction (XRD). In the whole, the present experiments show that the ferromagnetism in the microscale does not destroy superconductivity for LSCO cuprate in this kind of the matrix composites, and the intercalation of LSMO may lead to an electronic phase separation in LSCO with the hole rich and/or hole poor regions.

© 2011 Elsevier B.V. All rights reserved.

## 1. Introduction

In the recent years, interface properties of ferromagnets and superconductors have been one of the most interesting topics due to potential device applications in superconducting electronics [1–6]. In conventional s-wave superconductors, local magnetic moments break up spin-singlet Cooper pairs and hence strongly suppress the superconductivity (SC). Large numbers of research papers on the effects of impurities substitution on superconductivity show that a level of magnetic impurity of 1% only, can result in a complete loss of SC. However, it was found that the superconductivity can coexist with the “striped” antiferromagnetic order which is induced by an applied magnetic field in a cuprate superconductor [7]. Therefore, it is significant to find the intrinsic competition mechanism between superconductivity and magnetism. However, the relationship between the superconductivity and magnetism mentioned above has been mainly focused on La–Sr–Cu–O based system with a mixture of ferromagnetism (FM) metal. It is well known that the characteristics of  $\text{CuO}_2$  planes are essential to understand the unconventional superconductivity

and the anomalous transport behavior of normal state in cuprate superconductors. One is that the high superconducting transition temperature ( $T_{sc}$ ) superconductivity can be obtained by appropriate substitution of Sr for La in the form of  $\text{La}_{1.85}\text{Sr}_{0.15}\text{CuO}_4$  due to some hole-carriers introduced by Sr in  $\text{CuO}_2$  planes [8]. Another is that the superconductivity in  $\text{La}_{1.85}\text{Sr}_{0.15}\text{CuO}_4$  can be significantly suppressed by both the magnetic and nonmagnetic impurities doping on the Cu sites [1,2,9–18]. Here, to avoid the destruction of  $\text{CuO}_2$  planes in  $\text{La}_{1.85}\text{Sr}_{0.15}\text{CuO}_4$  with intercalation of ferromagnets, we have studied the influence of  $\text{La}_{2/3}\text{Sr}_{1/3}\text{MnO}_3$  (LSMO) on the superconductivity of  $\text{La}_{1.85}\text{Sr}_{0.15}\text{CuO}_4$  (LSCO) below the  $T_{sc}$ . The similar structural and transport properties of the manganite and cuprate powders have stimulated many attempt of building hybrid composite [19–22].  $\text{La}_{2/3}\text{Sr}_{1/3}\text{MnO}_3$  was chosen in this study due to the fact that it is a typical double exchange ferromagnetic compound with a high Curie temperature ( $T_{Curie} = 370\text{ K}$ ) owing to its very large one-electron bandwidth [23–27]. In order to clarify the interaction between superconductivity and magnetism, in this work, we successfully prepared a series of matrix composites with a stoichiometric formula of  $(\text{La}_{1.85}\text{Sr}_{0.15}\text{CuO}_4)_{1-x}(\text{La}_{2/3}\text{Sr}_{1/3}\text{MnO}_3)_x$  (LSCO/LSMO) by solid-state reaction method. The present system of LSCO/LSMO provides a good example for studying the effect of FM on superconductivity where the Cu–O planes are not destructed. In the whole, our experiments show that

\* Corresponding author.

E-mail address: [jczhang@staff.shu.edu.cn](mailto:jczhang@staff.shu.edu.cn) (J. Zhang).

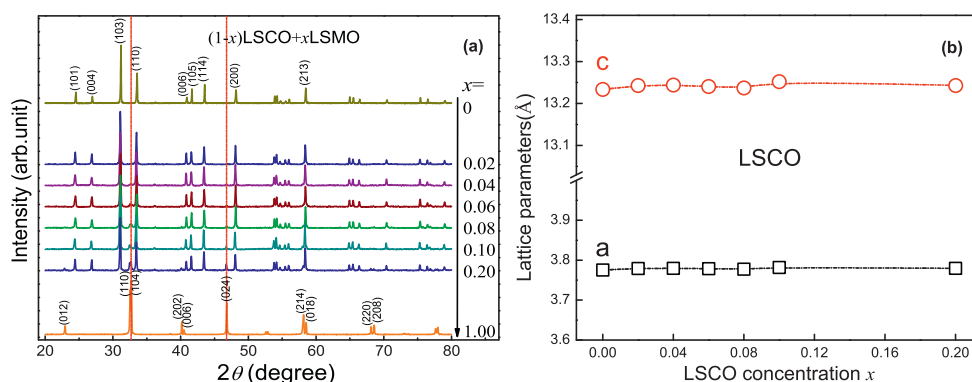


**Fig. 1.** (a) Room temperature X-ray diffraction pattern of LSMO, LSCO and their composites. Note that all the peaks are identified. (b) Variation in the lattice parameters (a and c) of LSCO with  $x$  for all the composites at room temperature.

the ferromagnetism in the microscale does not destroy superconductivity for LSCO cuprate in this kind of the matrix composites. The present results will be meaning to understand the interaction and coexistence mechanism between ferromagnetism and superconductivity in the matrix composites.

## 2. Samples and experiments

The matrix composites of  $(\text{La}_{1.85}\text{Sr}_{0.15}\text{CuO}_4)_{1-x}(\text{La}_{2/3}\text{Sr}_{1/3}\text{MnO}_3)_x$  ( $x = 0.00, 0.02, 0.04, 0.08, 0.10, 0.20$ ) were prepared from LSCO and LSMO polycrystalline powder, respectively. Here, polycrystalline samples of nominal composition  $\text{La}_{1.85}\text{Sr}_{0.15}\text{CuO}_4$  were firstly synthesized by the convenient solid state reaction method from heat treating stoichiometric quantities of high purity  $\text{La}_2\text{O}_3$ ,  $\text{SrCO}_3$ , and  $\text{CuO}$  powders at  $1000^\circ\text{C}$  for 20 h in air atmosphere. The heat treatment was repeated three times after grinding and repelletizing each time to ensure the homogeneity of the samples. At the same time, polycrystalline samples of nominal composition  $\text{La}_{2/3}\text{Sr}_{1/3}\text{MnO}_3$  was prepared by the solid state reaction of high purity  $\text{La}_2\text{O}_3$ ,  $\text{SrCO}_3$ , and  $\text{MnO}_2$ . The raw materials were mixed, pelletized and sintered at  $1000^\circ\text{C}$  for 12 h,  $1200^\circ\text{C}$  for 24 h and  $1350^\circ\text{C}$  for 24 h with intermediate grinding and repelletizing. Finally, the obtained powders of LSCO and LSMO were prepared by mixing 2, 4, 6, 8, 10 and 20 mol% of LSMO phase with 98, 96, 94, 92, 90 and 80 mol% of LSCO phase, respectively. To avoid the destruction of  $\text{CuO}_2$  planes in LSCO with intercalation of LSMO, we choose the low sintering temperature and short sintering time. Therefore, the composite mixtures were ultimately pressed into pellets at the pressure of 12 MPa/cm<sup>2</sup> and sintered at  $900^\circ\text{C}$  for 8 h to yield the final matrix composites.

The structural characterization was done by using the X-ray diffraction (XRD, Rigaku18 kW/MAX-2500 diffraction with  $\text{Cu-K}\alpha$  radiation) at room temperature in the  $2\theta$  range of  $(20-80^\circ)$  with a step of  $0.02^\circ$ . The surface morphology was observed by scanning electron microscopy (SEM). The magnetic measurements were performed by utilizing a vibrating sample magnetometer (VSM) in the temperature range from 2.5 to 380 K. The temperature dependent resistivity measurements were carried out using the standard four-probe method in a Physical Property Measurement System (PPMS) at a temperature range from 2.5 to 100 K. Silver paint was used to make electrical contacts on the sample and Cu wires were used as electrical leads. The experimental results are well repeatable on the structure and physical properties for all experimental samples.

## 3. Results and discussion

The room temperature powder XRD patterns of experimental samples for LSCO/LSMO matrix composites ( $x = 0.00, 0.02, 0.04,$

0.06, 0.08, 0.10, 0.20, 1.00) are shown in Fig. 1(a). The XRD pattern of the parent LSCO can be indexed to a tetragonal unit cell with lattice parameters  $a = 3.7754 \text{ \AA}$  and  $c = 13.2333 \text{ \AA}$  and that of LSMO to an orthorhombic unit cell with lattice parameters  $a = 5.4907 \text{ \AA}$ , and  $c = 13.3245 \text{ \AA}$  using the standard least-squares refinement of the patterns (in Table 1). These results of XRD patterns in Fig. 1(a) show well that the characteristics of matrix composites and the phase coexistence of LSCO cuprates and LSMO manganites are compatible with each other for the composite samples, indicating no observable chemical reaction between the two components during the final calcination and the  $\text{CuO}_2$  planes are not broken. With the increment of LSMO content, the intensity of the LSMO peaks gradually increases, although the intensity of the LSCO peaks barely decreases. Using the standard least-squares refinement of the patterns, the lattice parameters for both phases have been calculated except for the composites beyond the resolution limit of the XRD ( $x = 0.02, 0.04$ ). Fig. 1(b) shows the lattice parameters of LSCO,  $a$  and  $c$ , are scarcely changed with increasing LSMO content for all the samples. Taking into account the scattering, the particle size, depth of sample packing and packing method for the sample may result in the fluctuation of  $a$  and  $c$ .

SEM of all the composites was taken in order to obtain an idea about the distribution of LSMO in LSCO. The representative SEM micrographs of LSCO/LSMO matrix composites with  $x = 0.04$  and  $x = 0.20$  are shown in Fig. 2, respectively. Moreover, energy dispersive X-ray (EDX) spectra of the doped composite for  $x = 0.04$  and  $x = 0.20$  shows the manganese peak along with La, Sr, Cu and O peaks, which also indicates that the manganese content of LSMO rises with increasing  $x$ .

Fig. 3 shows the temperature dependence of the reduced resistivity and  $x$  dependence of  $T_{\text{sc-off}}$  (the off-set point) in the temperature range of 2.5–100 K for the LSCO/LSMO matrix composites under zero field, in which a normalized resistivity is used by  $\rho(T)/\rho(T = 40 \text{ K})$  to reveal the distinct changing tendency of the resistivity with increasing the temperature. For all the samples, the resistivity decreases abruptly at about 38 K, manifesting the occur-

**Table 1**

The lattice parameters of LSCO and LSMO ( $a$  and  $c$ ),  $T_{\text{sc-off}}$  and  $M$  (100 K) for LSCO/LSMO composites (defined in text).

$x$ (mol)	LSCO		LSMO		$T_{\text{sc-off}}$ (K)	$M$ (100 K) (emu/g)
	$a$ (Å)	$c$ (Å)	$a$ (Å)	$c$ (Å)		
0	3.7754	13.2333	–	–	37	0.0055
0.02	3.7791	13.2423	–	–	28	0.0604
0.04	3.7797	13.2440	–	–	25	0.1143
0.06	3.7789	13.2401	5.4982	13.2322	23	0.1871
0.08	3.7777	13.2372	5.4885	13.2439	21	0.2850
0.10	3.7818	13.2519	5.5013	13.2684	19	0.4207
0.20	3.7798	13.2430	5.4947	13.2466	8	0.9869
1	–	–	5.4907	13.3245	–	–

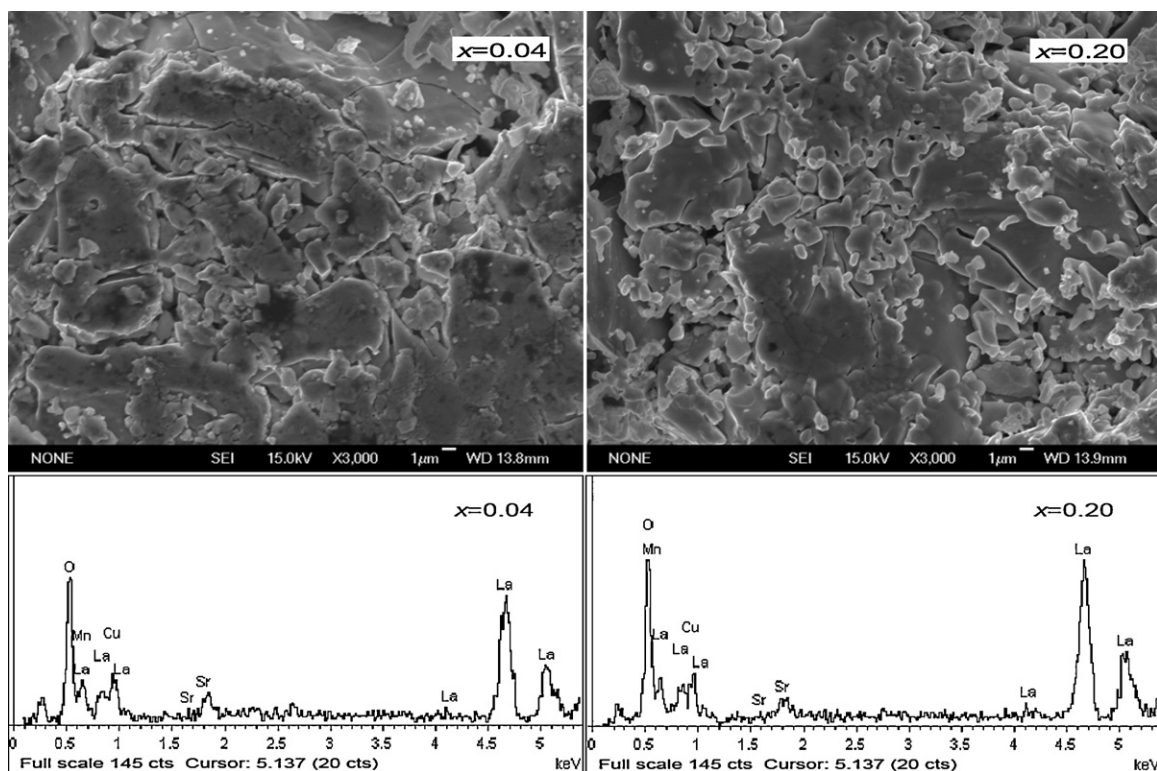


Fig. 2. Scanning electron micrographs and EDX spectra of LSCO/LSMO composite with  $x=0.04$  and  $x=0.20$ .

rence of superconductivity, and the superconducting transition get broadened upon increasing  $x$ . In order to compare the values of the superconducting transition temperature ( $T_{sc}$ ) more clearly,  $T_{sc}$  is marked at two points commonly [28], the on-set point  $T_{sc-on}$  and  $T_{sc-off}$ .  $T_{sc-on}$  is defined as the crossing point of an extended line from the steepest slope of transition and an extracted line of the normal state while  $T_{sc-off}$  is the crossing point of the extended line and  $x$ -axis. The difference between  $T_{sc-on}$  and  $T_{sc-off}$  is defined as the

transition width  $\Delta T_{sc}$ , which is an indication of the homogeneity of hole-distribution in the sample. The narrower, the more homogeneous the sample is. We pay more attention to the  $T_{sc-off}$  in our study because of the negligible shift (not shown here) of  $T_{sc-on}$  unified as 40 K for all the composite samples. The variety of  $T_{sc-off}$  can indicate the variety of  $\Delta T_{sc}$  with increasing  $x$  observably. The inset of Fig. 3 (at the right bottom) shows that  $T_{sc-off}$  decreases from 28 to 8 K with increasing the mole fraction of LSMO from 0.02 mol to 0.20 mol, which is almost consistent with previous experimental results [29]. In our study, it is very interesting that the effect of FM on superconducting suppression is less stronger than the results from Hsu et al. [30]. From the results of XRD, we believe that there is no any chemical reaction between the composites which may lead to such drastic reduction in the superconducting volume fraction and the change in resistivity behavior at low temperature. Also, we think that if there is a chemical reaction between the composites there should have been a reduction in  $T_{sc-off}$ . These results suggest that something should be happening at the microscopic level in LSCO upon intercalation with LSMO.

As we all know, LSMO manganites are ferromagnetic when the temperature is lower than the magnetic phase transition temperature (Curie temperature,  $T_{Curie}$ ). It will cause the breaking of Cooper pairs in the interface between LSMO and LSCO. Therefore the superconductivity suppression in the composites indicates the interaction between superconductivity and magnetism in the grain boundary of LSCO/LSMO. The grain boundary effects like interface disorder, strain and interdiffusion have been taken into account in other study [31]. We hypothesize that one of the possible reasons for such a change in the resistivity behavior can be that the intercalation of LSMO may be leading to an electronic phase separation in LSCO with hole rich and hole poor regions. If that is the case the observed decrease in the superconducting volume fraction can be explained to be due to the absence of superconductivity in the hole poor regions of LSCO. Due to low sintering temperature and short sintering time during the final calcination, the interaction between

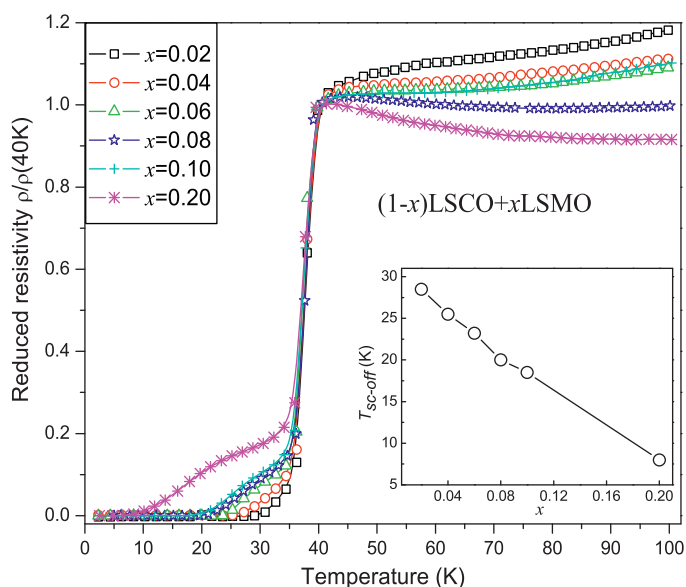
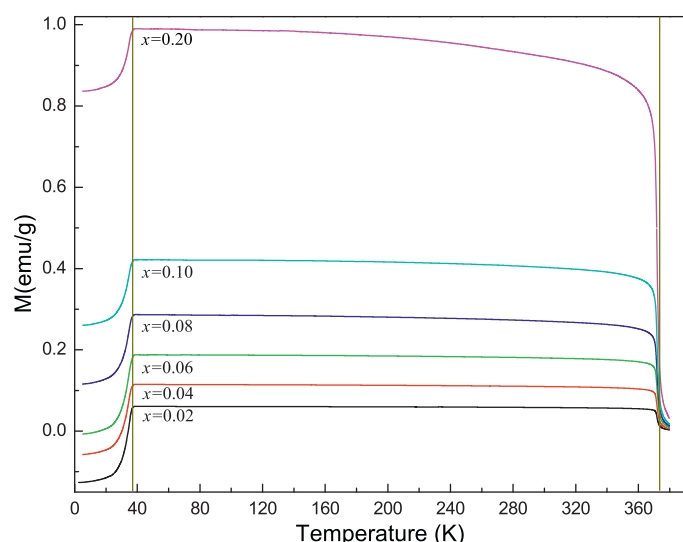


Fig. 3. Details of the temperature dependence of reduced resistivity under a zero field in a low temperature region of 2.5–100 K for LSCO with the various doped of LSMO ( $x=0.02, 0.04, 0.06, 0.08, 0.10, 0.20, 1.00$ ). The inset is the superconducting transition temperature  $T_{sc-off}$  versus  $x$ .



**Fig. 4.** Magnetization  $M$  versus temperature  $T$  for all the samples with field-cooled ZFC modes (2.5–380 K). Lines are guides for the eyes. Superconducting volume fraction decreases drastically on intercalation with LSMO whereas  $T_{\text{Curie}}$  is almost unaffected.

the superconductivity and magnetism grows faint and the electronic phase separation becomes more slowly. These results also suggest a competition between magnetism and superconductivity in LSCO/LSMO, although the proximity effect cannot be established unambiguously in the polycrystal composites. Descent of the critical temperature of LSCO can due to pair-breaking by carriers of LSMO injected into the grain boundary of LSCO/LSMO.

Fig. 4 shows the magnetization ( $M$ ) versus temperature ( $T$ ) ( $M$ – $T$ ) for all the samples in field-cooled (FC) modes (under 100 Oe field). The left vertical line at 38 K indicates  $T_{\text{sc-on}}$  change hardly which is consistent with the result in Fig. 3, at the same time the right vertical line at 374 K represents Curie temperature ( $T_{\text{Curie}}$ ) of LSMO manganites. Based on these  $M$ – $T$  curves, there is a monotonic increase in the magnetization with increase in  $x$  for all the samples. The magnetization results testify that existence of LSMO manganites particle leads to an increase of magnetization, which is caused not only by dilution effect, but also by its interaction with the neighboring FM particles. The two visible transition points in the  $M$ – $T$  curves from 2.5 K to 380 K for all the composites are due to the fact that the paramagnetic to ferromagnetic phase transition for LSMO and superconductivity phase transition for LSCO are intrinsic and intragrain property, respectively. It is also shown that there is no reaction between LSCO and LSMO since all the  $T_{\text{Curie}}$  shift hardly with increasing  $x$ . The previous magnetism investigation results indicate that  $T_{\text{Curie}}$  of LSMO manganites will shift to lower temperature when they border upon superconductors due to proximity effects [28]. However,  $T_{\text{Curie}}$  of LSMO hardly changes in every matrix composite when LSMO enter LSCO compound in our study, if LSCO and LSMO play their roles, respectively in the composites. It also shows that there is the coexistence distinctly between LSCO and LSMO in the matrix composites at the temperature range from 2.5 K to 380 K.

Hysteresis loops ( $M$ – $H$ ) measured below ( $T=4$  K) and above the superconducting onset ( $T=40$  K) are shown for typical samples of LSCO/LSMO matrix composites with  $x=0.02$ ,  $x=0.08$  and  $x=0.20$  in Fig. 5. For the samples at 40 K, the clear observation of the magnetic properties shows that the ferromagnetic hysteresis characteristic in the present LSCO/LSMO matrix composites, and there is a linear increase in the saturation magnetization ( $M_s$ ) with increasing  $x$ . It is also clearly observed that there is a central peak around zero field for the LSCO/LSMO matrix composites with  $x=0.02$  at

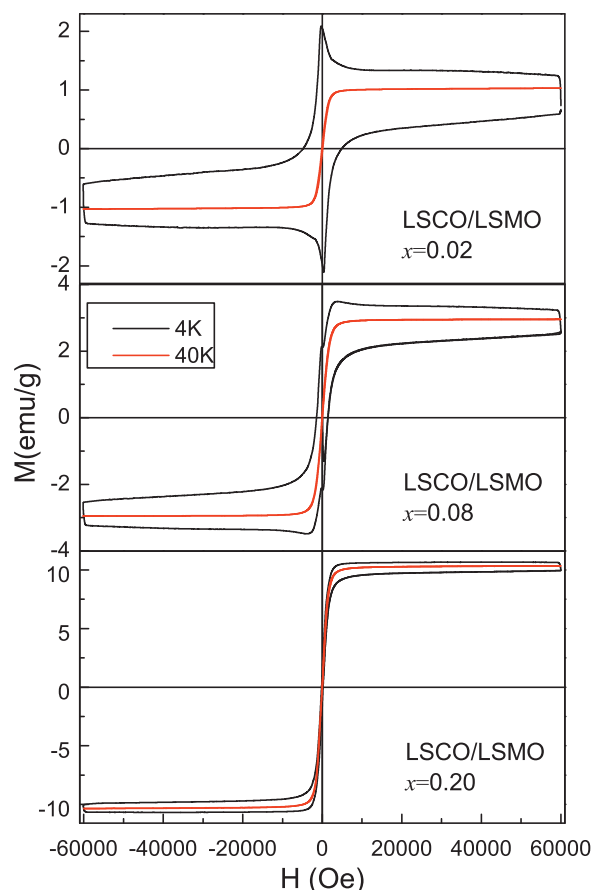


**Fig. 5.** Magnetization loops for LSCO/LSMO composites ( $x=0.02$ ,  $x=0.08$  and  $x=0.20$ ) measured at 4 K and 40 K, respectively.

4 K, which demonstrates characteristic superconducting-like hysteresis loop as expected from parent LSCO. With increasing  $x$ , the central peak around zero field die down gradually, which is due to the fact that the hole-distribution become less homogeneous in the composites with the intercalation of LSMO in the grain boundary. For the composite of LSCO/LSMO with  $x=0.2$  at 4 K, the  $M$ – $T$  presents typical ferromagnetic hysteresis loop shape. These magnetic hysteresis loops in different temperature ranges show a complex behavior that is due to the interplay between Meissner currents in the polycrystalline LSCO and the magnetic fields present in the polycrystalline LSMO.

#### 4. Conclusion

We have successfully synthesized the matrix composites of  $(\text{La}_{1.85}\text{Sr}_{0.15}\text{CuO}_4)_{1-x}(\text{La}_{2/3}\text{Sr}_{1/3}\text{MnO}_3)_x$  for  $x=0-0.20$  mol by a conventional solid-state reaction method and the temperature dependent electrical and magnetic properties of the samples are investigated. The resistive transport properties exhibit a gradual suppression of the superconductivity as increasing LSMO content. Although intercalation of LSMO in LSCO does not change the onset of superconducting transition temperature considerably, the offset of superconducting transition temperature decreases drastically with increase in  $x$ . It is proposed that the intercalation leads to a hole segregation in the grain boundary of LSCO/LSMO, which may be the cause for the observed broad  $\Delta T_{\text{sc}}$ . The magnetic properties present that there are coexistence and competition between the magnetism and superconductivity where the  $\text{CuO}_2$  planes are intact. The saturation magnetization increases monotonically with increase in  $x$ , indicating the gradual increase of the mag-

netic phase. The ferromagnetic–paramagnetic transition of LSMO is clearly observed from  $M-T$  and  $T_{\text{Curie}}$  of LSMO change hardly for all the composites, because there are no reaction between LSMO and LSCO. The present experiments show that the ferromagnetism does not destroy superconductivity for LSCO cuprate in this kind of the matrix composites. Therefore, the  $\text{CuO}_2$  plane is very important to understand the relationship between the superconductivity and magnetism, but it is not the only factor. The result will be meaning to understand the interaction and coexistence mechanism between ferromagnetism and superconductivity.

## Acknowledgments

This work is supported by the National Natural Science Foundation of China (NSFC, Grant No. 11074163, 50932003), Program for Changjiang Scholars and Innovative Research Team in University (Grant No: IRT0739), The Science & Technology Committee of Shanghai Municipality (Grant No.08dj1400202), Special Research Foundation for the Doctoral Discipline of University (Grant No. 200802800003), the Science and Technology Innovation Fund of the Shanghai Education Committee (Grant No. 09ZZ95).

## References

- [1] H. Wu, S. Tan, W.X. Wang, Y.H. Zhang, Phys. Rev. B 71 (2005) 144520.
- [2] J.T. Xu, S. Tan, L. Pi, Y.H. Zhang, J. Appl. Phys. 104 (2008) 063914.
- [3] I. Felner, U. Asaf, Superlattice Microstruct. 24 (1998) 99.
- [4] H. Eisaki, H. Takagi, Phys. Rev. B 50 (1994) 647.
- [5] T.E. Grigereit, J.W. Lynn, Q. Huang, A. Santoro, Phys. Rev. Lett. 73 (1994) 2756.
- [6] A. Yazdani, B.A. Jones, C.P. Lutz, M.F. Crommie, D.M. Eigler, Science 275 (1997) 1767.
- [7] B. Lake, H.M. Rønnow, N.B. Christensen, G. Aeppli, K. Lefmann, D.F. McMorrow, P. Vorderwisch, P. Smeibidl, N. Mangkorntong, T. Sasagawa, et al., Nature 415 (2002) 299.
- [8] D.C. Johnston, F. Borsa, J.H. Cho, J. Alloys Compd. 207 (1994) 12.
- [9] J.M. Tarascon, L.H. Greene, P. Barboux, W.R. McKinnon, G.W. Hull, T.P. Orlando, K.A. Delin, S. Foner, E.J. McNiff, Phys. Rev. B 36 (1987) 8393.
- [10] P.W. Anderson, Phys. Rev. Lett. 3 (1959) 325.
- [11] G. Xiao, M.Z. Cieplak, J.Q. Xiao, C.L. Chien, Phys. Rev. B 42 (1990) 8752.
- [12] R. Fehrenbacher, Phys. Rev. Lett. 77 (1996) 1849.
- [13] S.K. Agarwal, R. Suryanarayanan, O. Gorochoy, V.N. Moorthy, A.V. Narlikar, Solid State Commun. 79 (1991) 857.
- [14] C.J. Zhang, Y.H. Zhang, Phys. Rev. B 68 (2003) 54512.
- [15] C.X. Wang, Y.P. Sun, Z. Qu, Y.H. Zhang, Phys. Rev. B 73 (2006) 144518.
- [16] R. Kilian, S. Krivenko, G. Khaliullin, P. Fulde, Phys. Rev. B 59 (1999) 14432.
- [17] J.X. Zhu, C.S. Ting, Phys. Rev. B 64 (2001) 060501.
- [18] A. Polkovnikov, S. Sachdev, M. Vojta, Phys. Rev. Lett. 86 (2001) 296.
- [19] X.H. Li, Y.H. Huang, Z.M. Wang, C.H. Yan, Appl. Phys. Lett. 81 (2002) 1313.
- [20] J. Chakhalian, J.W. Freeland, H.U. Habermeier, G. Cristiani, G. Khaliullin, M. van Veenendaal, B. Keimer, Science 318 (2007) 1114.
- [21] J.W. Freeland, J. Chakhalian, H.U. Habermeier, G. Cristiani, B. Keimer, Appl. Phys. Lett. 90 (2007) 242502.
- [22] M. van Zalk, M. Veldhorst, A. Brinkman, J. Aarts, H. Hilgenkamp, Phys. Rev. B 79 (2009) 134509.
- [23] G. Van Tendeloo, O.I. Lebedev, M. Hervieu, B. Raveau, Rep. Prog. Phys. 67 (2004) 1315.
- [24] Z.F. Zi, Y.P. Sun, X. Bzhu, C.Y. Hao, X. Luo, Z.R. Yang, J.M. Dai, W.H. Song, J. Alloys Compd. 477 (2009) 414.
- [25] I.A. Abdel-Latif, A. Hassen, C. Zybilla, M. Abdel-Hafiez, S. Allam, T. El-Sherbini, J. Alloys Compd. 452 (2008) 245.
- [26] P.K. Siwach, R. Prasad, A. Gaur, H.K. Singh, G.D. Varma, O.N. Srivastava, J. Alloys Compd. 443 (2007) 26.
- [27] X.B. Zhu, D.Q. Shi, L. Zhang, Y.P. Sun, W.H. Song, L. Wang, T.M. Silver, S.X. Dou, J. Alloys Compd. 459 (2008) 83.
- [28] J.G. Lin, D. Hsu, M.Y. Song, C.H. Chiang, W.C. Chan, J. Appl. Phys. 107 (2010) 09E130.
- [29] H. Schmidt, H.F. Braun, Phys. Rev. B 55 (1997) 8497.
- [30] D. Hsu, T. Greetha Kumary, L. Lin, J.G. Lin, Phys. Rev. B 74 (2006) 214504.
- [31] W.S. Tan, L. Yang, X.S. Wu, S.S. Jiang, T.L. Kam, J. Gao, J. Wang, Z.H. Wu, Physica C 384 (2003) 437.